

TokenPure: Watermark Removal through Tokenized Appearance and Structural Guidance

Pei Yang¹ Yepeng Liu² Kelly Peng¹ Yuan Gao¹ Yiren Song^{1,3}†

¹First Intelligence ²University of California, Santa Barbara ³National University of Singapore

Abstract

In the digital economy era, digital watermarking serves as a critical basis for ownership proof of massive replicable content, including AI-generated and other virtual assets. Designing robust watermarks capable of withstanding various attacks and processing operations is even more paramount. We introduce TokenPure, a novel Diffusion Transformer-based framework designed for effective and consistent watermark removal. TokenPure solves the trade-off between thorough watermark destruction and content consistency by leveraging token-based conditional reconstruction. It reframes the task as conditional generation, entirely bypassing the initial watermark-carrying noise. We achieve this by decomposing the watermarked image into two complementary token sets: visual tokens for texture and structural tokens for geometry. These tokens jointly condition the diffusion process, enabling the framework to synthesize watermark-free images with fine-grained consistency and structural integrity. Comprehensive experiments show that TokenPure achieves state-of-the-art watermark removal and reconstruction fidelity, substantially outperforming existing baselines in both perceptual quality and consistency. Code is released at <https://github.com/YoungP2001/TokenPure>.

1. Introduction

Currently, the explosive development of generative models [71], such as Stable Diffusion [67] and LLaVA [44], has significantly lowered the barrier to AI creation, leading to a surge in AI-generated content output. Against this backdrop, digital watermarking [25, 43, 49, 106] has become increasingly crucial as a key tool for tracking the source of AI content [10, 11, 24, 33, 45, 47], protecting data copyright [8, 23, 48, 53, 94], defending against deepfakes [88], and ensuring information transparency.

Robustness lies at the core of watermarking effectiveness, ensuring reliable detection and integrity even in the

face of diverse transformations or adversarial attacks [2, 3, 21, 76, 80, 85, 90]. However, with the rapid advancement of AI techniques [20, 98, 102, 105], particularly generative models, watermark robustness faces unprecedented challenges in maintaining its reliability and resilience. Therefore, investigating an effective watermark removal method serves as a stress test for current watermarking schemes, revealing their vulnerabilities and guiding the development of future methods with higher robustness standards.

The robustness of existing image watermarking methods varies with the degree of perturbation introduced to either the original image [12, 16, 81, 108] or the image generation process [10, 11, 17, 85]. Low-perturbation watermarks [17, 95, 108], due to their small perturbation, e.g., small ℓ_2 distance, of the original content, have relatively limited resistance against naive image manipulation. High-perturbation watermarks [10, 11, 33, 46, 70, 81, 107] usually introduce substantial modifications to the image in either pixel space or latent space, making it more difficult for adversaries to fully remove the underlying watermark information without destroying the semantics of original images.

Recent advances in generative models have spurred progress in watermark removal methods [1, 46, 107]. These methods leverage powerful generative models to regenerate the watermarked image, thereby eliminating the embedded watermark signal. These approaches excel at disrupting many low-perturbation watermarks, yet their limitations become evident in handling complex scenarios. For instance, [107] introduces a regeneration attack that leverages the characteristic noising process of diffusion models, effectively destroying low-perturbation watermarks by iteratively adding noise to the latent representation. However, it performs poorly on high-perturbation watermarks. [1] seeks to achieve more thorough watermark removal by cascading multiple regeneration iterations. While this strategy improves removal performance to some extent, it also introduces noticeable image degradation and artifacts due to the excessive noising steps. To improve the trade-off between attack performance and image quality, [46] proposes a controllable regeneration method that reconstructs watermark-free images from clean initial noise using a diffusion model.

† Corresponding author.

While this approach substantially enhances removal effectiveness, it also introduces noticeable color and texture deviations in the reconstructed images, compromising visual consistency.

Regenerating a watermarked image from clean noise can effectively eliminate the embedded watermark information, but coarse-grained control often results in noticeable inconsistencies in the reconstructed image. This raises an important question: how can we further enhance reconstruction consistency while still ensuring complete removal of watermark signals?

In this paper, we propose a fine-grained token level regeneration method. We find that heavy compression or high-frequency suppression (e.g., low-token representations, visual prompt encoding [65, 93]) significantly weakens watermark signals, revealing noise-level embedding vulnerabilities. Additionally, token-level units provide finer-grained reconstruction cues. Motivated by this, we propose TokenPure, a Diffusion Transformer-based conditional framework that removes watermarks without initial watermark-carrying noise. We further compress watermark-agnostic edge information to guide reconstruction via complementary content priors, ensuring thorough removal and structural consistency. Instead of direct image-to-image translation, TokenPure reformulates the task as conditional generation guided by two complementary token branches: (1) an Appearance Adapter that compresses watermarked images into compact visual tokens to capture color and texture cues; (2) a Layout Controller that extracts edge information and encodes it into structural tokens via VAE to preserve geometry. These branches jointly condition the diffusion transformer (DiT) [63] to synthesize watermark-free images from visual-structural priors, effectively disentangling watermark signals from the visual content.

Extensive experiments across multiple benchmarks demonstrates that TokenPure achieves superior de-watermarking precision and reconstruction fidelity. It delivers perceptually sharper, more consistent results, moving beyond quantitative metrics.

Our contributions can be summarized as follows:

- A novel Diffusion Transformer-based de-watermarking framework, TokenPure, is proposed to enable non-watermark image reconstruction.
- An Appearance Adapter and a Layout Controller are designed to implement complementary visual-structural conditioning, jointly facilitating accurate and interpretable image purification.
- Comprehensive quantitative and qualitative evaluations are performed, demonstrating that TokenPure attains state-of-the-art performance in both watermark removal efficacy and reconstruction consistency.

2. Relate works

2.1. Image Watermarking Methods

Image watermarking provides a reliable mechanism for ownership verification and content traceability. Early approaches embed watermark information directly into images [7, 34, 68]. With the rise of large generative models such as Stable Diffusion [67], watermarking can now be seamlessly integrated during content generation. Existing approaches can be broadly divided into *post-hoc* and *in-generation* watermarking. Post-hoc methods embed signals after image creation via encoder-decoder architectures [81, 108], optimization [16], or transform-based embedding [12]. In contrast, in-generation methods [87] modify the generative process itself, such as altering initial noise [11, 60, 85], manipulating latent decoders [10, 17] or semantic embedding [4, 40]. We evaluate our proposed approach under both categories to ensure comprehensive coverage.

2.2. Image Watermark Removal Methods

The robustness of watermarks is typically assessed through *removal attacks* [31, 37, 42, 89], including editing, regeneration, and adversarial types. Editing attacks involve simple manipulations—cropping, compression, rotation, or noise injection—simulating common real-world distortions. Most watermarking methods remain stable under such perturbations. Recently, *regeneration attacks* [62, 70, 107] propose to remove watermarks by re-synthesizing images through the denoising process of pretrained diffusion models or VAE decoding. These approaches effectively erase weakly embedded signals but perform poorly against high-perturbation watermarking schemes. Alternatively, *adversarial attacks* [36, 52, 70, 109] optimize pixel-level perturbations to deceive detectors, but they require prior knowledge of the watermarking algorithm or model access, making them costly and impractical. In this work, we focus on the regeneration-based paradigm and propose a more fine-grained watermark removal strategy to better ensure consistency.

2.3. Diffusion Models

Diffusion probabilistic models [29, 74] generate data by iteratively denoising Gaussian noise and have achieved remarkable success in image synthesis [63, 67], editing [5, 27, 101, 103], and 3D generation [64]. Stable Diffusion [67] serves as a representative model, employing a UNet backbone to achieve high-quality text-to-image generation and inspired subsequent work [9, 75, 101, 103]. Controllability [54–59] has since improved via auxiliary modules such as ControlNet [41, 96] and T2I-Adapter [61], which use multimodal conditions like depth or segmentation. Subject-driven generation further evolved from fine-

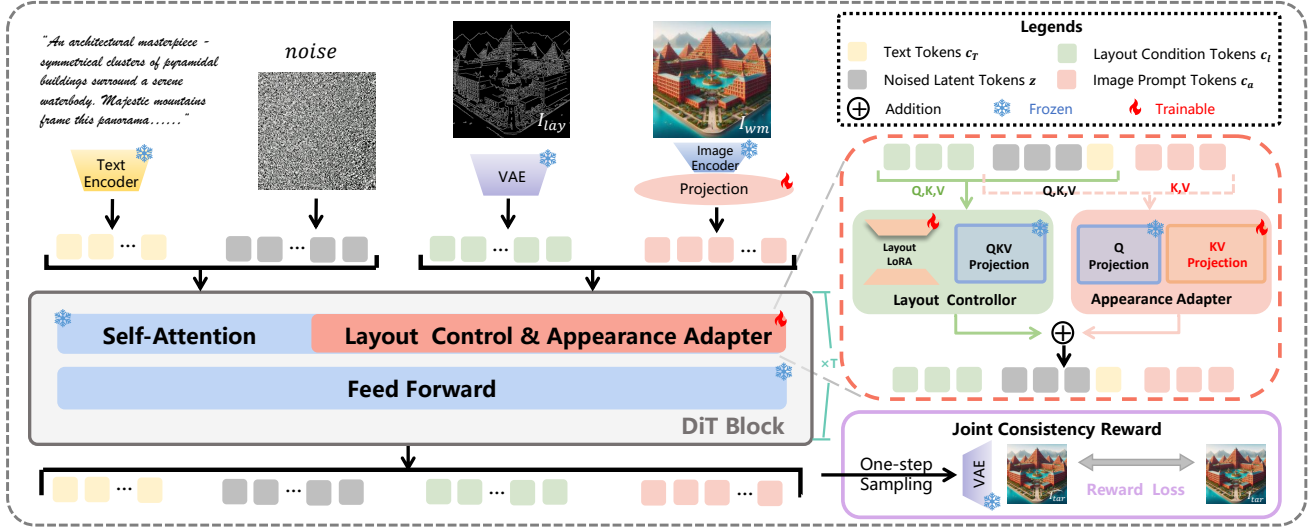


Figure 1. The illustration of TokenPure framework. It takes text, noise, the layout representation I_{lay} (from edge detection and VAE encoding) of the watermarked image I_{wm} , and image prompt tokens (from the Image Encoder and Projection of I_{wm}) as inputs. Within the DiT Block, the Self-Attention and Feed Forward modules process these tokens, while the Layout Control & Appearance Adapter branch integrates spatial structure and visual details. The Layout Controller uses a LoRA module to optimize layout tokens’ QKV projection, and the Appearance Adapter performs trainable KV projection on image prompt tokens to interact with the Q projection of text and noise tokens via multimodal attention. Finally, the Joint Consistency Reward mechanism refines the result through one-step sampling and pixel-level reward loss, ensuring the reconstructed image’s consistency with the original.

tuning-based personalization [18, 30, 38, 69, 99, 100] to fine-tuning-free approaches [91, 99], offering diverse trade-offs between adaptability and efficiency. Recently, the Diffusion Transformer [63] has emerged as a key advancement, replacing the conventional UNet with a highly scalable Transformer architecture operating directly on latent tokens [19, 22, 32, 35, 51, 72, 73, 77–79, 82, 84, 104]. Building upon these advances, we design a controllable diffusion transformer-based framework, enabling precise de-watermarking through token-level conditioning.

3. Method

3.1. Overall Architecture

Our framework, **TokenPure**, is built upon a dual-branch Diffusion Transformer architecture designed to reconstruct watermark-free images from watermarked image tokens without relying on initial noise. As illustrated in Fig. 1, the system consists of two complementary branches: (1) an *Appearance Adapter* Branch that provides visual appearance cues, and (2) a *Layout Controller* Branch that encodes geometric and structural information. Both branches interact through multimodal attention within a unified diffusion backbone based on the Flux Transformer.

3.2. Appearance Adapter

Given a watermarked image I_{wm} , we first extract its feature sequence using a pretrained image encoder SigLIP without applying any noise perturbation. Unlike Flux-IP-Adapter, it only uses the pooled feature as visual prompts, which are more suitable for the classification task. Particularly, we extract the token-level feature of the last hidden layer in SigLIP [93] as the input of our Appearance Adapter, which preserves richer semantic details. The extracted latent features are then projected through a series of linear modules and activators, which map them into a compact set of visual tokens c_a . These tokens capture color, texture, and fine-scale appearance cues while filtering out high-frequency watermark residuals. The visual tokens are concatenated with the text tokens c_T from the frozen Flux model’s T5 [66] text encoder and random noise tokens z_t sampled from a Gaussian distribution, forming a multimodal token sequence.

A key challenge lies in how to effectively embed semantic features while injecting them without disrupting the prior relationships among the original multimodalities. We have designed a novel Multimodal attention mechanism, which adopts the query Q (including text and noise tokens) from the original DiT module and their frozen Q projection weights (W_q). Meanwhile, we create a new key-value (K_A, V_A) attention projection module for our visual tokens

(c_a). The output of the new attention, denoted as Z_A , is computed as follows:

$$Z_A = \text{Attention}(Q, K_A, V_A) = \text{Softmax} \left(\frac{QK_A^\top}{\sqrt{d}} \right) V_A, \quad (1)$$

where $Q = (z_t, c_T)W_q$, $K_A = c_aW_k$, $V_A = c_aW_v$ are the query, key, and values matrices of the attention operation respectively, and W_q, W_k, W_v are the corresponding weight projection matrices. (z_T, c_t) represents the concatenation of z_t and c_T .

Through a Multimodal Attention mechanism, the Diffusion Transformer integrates the textual condition with the appearance embedding, effectively grounding the reconstruction in clean, semantically aligned visual priors.

3.3. Layout Controller

Although semantic branches can achieve semantic consistency between the generated content and the original watermark image through text guidance and high-level semantic features, the inherent Transformer-based sequence modeling characteristic of DiT is prone to problems such as spatial topological structure blurring (such as continuous object edges and distortion of local area geometric relationships) when processing image generation, which is particularly prominent in image reconstruction.

To address this, the Layout Controller branch focuses on the structural aspect of the input, including low-dimensional geometric information such as edge contours and regional boundaries, which can directly act on the token sequence modeling process of DiT. Unlike the conventional control network with redundant parameters and computational overhead, our method integrates the layout condition into the FLUX architecture through a lightweight Low-Rank Adaptation (LoRA) [30] Module. We first perform edge detection on the watermarked image to extract its layout representation, denoted as I_{lay} . This layout is encoded through a Variational Autoencoder (VAE) to obtain a set of *layout tokens* c_l that describe the geometric arrangement of the elements of the scene. The layout tokens are then concatenated directly with the denoising latent tokens of the diffusion process. The new QKV projection operations are unmodified as:

$$Q_L, K_L, V_L = Q + \Delta Q_L, K + \Delta K_L, V + \Delta V_L, \quad (2)$$

where Q, K, V are computed by frozen QKV projection in Flux architecture, and $\Delta Q_L, \Delta K_L, \Delta V_L$ are trainable low-rank matrices for each layer. Finally, the output Z_L of Layout Controller is defined as follows:

$$Z_L = \text{Attention}(Q_L, K_L, V_L) = \text{Softmax} \left(\frac{Q_L K_L^\top}{\sqrt{d}} \right) V_L. \quad (3)$$

Ultimately, these clean layout tokens act as fine-grained spatial priors for the transformer. This enables the model to maintain semantic consistency while accurately capturing edge topology and local spatial relationships, thereby effectively mitigating the dispersion of DiT spatial structures during generation.

3.4. Joint Dual-Branch Reconstruction

We fuse the Layout Controller attention output Z_L with the visual attention output Z_A (from the Appearance Adapter) before passing it to the Feed Forward module:

$$Z = Z_L + \alpha \cdot Z_A, \quad (4)$$

where α serves as a tunable scalar parameter that modulates the contribution of the visual prompt to the fused output. During diffusion denoising, the Appearance Adapter guides the model toward accurate local texture restoration, while the Layout Branch enforces global geometric stability. By jointly optimizing both branches under shared latent supervision, TokenPure achieves robust watermark removal and superior reconstruction fidelity.

To further enhance cross-branch coherence, we introduce a *Joint Consistency Reward* mechanism, allowing mutual refinement of structure and visual cues across time steps. During the training process, it adds noise to the unwatermarked image tokens z_0 and executes the forward diffusion process to obtain the noisy image tokens z'_t . Considered that the flow trajectory used in FLUX.1-dev is rectified flow (ReFlow), this is a simple diffusion trajectory: $z_t = (1-t)z_0 + t\epsilon$, where $z_0 \sim p_0$, $t \in [0, 1]$ and $\epsilon \sim N(0, 1)$. Since it defines the forward process as a straight path between the data distribution and the noise distribution, the learned velocity field $v_\theta(z_t, t)$ is used to directly map z_t to the target distribution during single-step sampling theoretically. The single-step sampling formula can be defined as:

$$z'_0 = \frac{z_t - t \cdot v_\theta(z_t, c_T, c_a, c_l, t)}{1-t}, \quad (5)$$

The core is to modify the linear interpolation path through the velocity field to achieve single-step denoising from the noisy state z_t to the generated tokens z'_0 . Particularly, When the added noise ϵ is small, the target image tokens z_0 can be similar to z'_0 .

Then, we directly decode cleaned tokens z'_0 into de-watermarked image I_{tar} for reward fine-tuning and calculate the reward consistency loss in the pixel space:

$$L_{re} = L(I_{tar}, \hat{I}_{tar}) = \frac{1}{H \times W} \sum_{i=1}^H \sum_{j=1}^W \left(z_{0(i,j)} - z'_{0(i,j)} \right)^2, \quad (6)$$

where H and W represent the height and width of the image I_{tar} and \hat{I}_{tar} respectively, and $H \times W$ denotes the total

number of pixels. In the reward fine-tuning stage, the pre-trained DiT model are frozen, and only dual branch networks are updated. This ensures that the generation capability of the model is not affected.

Finally, the loss is the combination of diffusion training loss L_{diff} and the reward loss:

$$L_{total} = \begin{cases} L_{diff} + \lambda \cdot L_{re}, & \text{if } t \leq t_{thre}, \\ L_{diff}, & \text{otherwise,} \end{cases} \quad (7)$$

where t_{thre} denotes the timestep threshold and λ controls the strength of reward. The diffusion loss L_{diff} enforces consistency in data distribution, while the reward loss L_{re} imposes constraints on pixel-level consistency. These two losses complement each other, enabling the model to purify latent representations while maintaining consistent spatial alignment, leading to state-of-the-art (SOTA) performance in both de-watermarking accuracy and visual consistency.

4. Experiment

4.1. Experimental Setting

Experimental Setup Our model is initialized with the frozen FLUX.1-dev [39] (DiT architecture), trained on 4 H20 GPUs for 100,000+ iterations with an accumulated batch size of 4. We use the AdamW optimizer [50] with bfloat16 mixed-precision training and an initial learning rate of 1×10^{-4} . The Appearance Adapter Module employs SigLIP as the visual prompt encoder, with compressed features output via a two-layer linear projection network and GELU activation [26]. The Layout Controller Module uses LoRA (rank=128) for efficient fine-tuning, preserving pre-trained generation capabilities. All inference is conducted on a single H20 GPU.

Dataset and Benchmark For the joint training of the Appearance Adapter and Layout Controller, we use 10 million image-text pairs from LLaVA-NeXT-Data, Dalle3 1 Million+ High Quality Captions [15], and Conceptual 12M (CC12M) [6]. For testing watermark attack performance, we construct a test dataset with 1000 images (synthetic/real from Echo-4o-Image [92] and ImageNet [13]) and 1000 GPT-4o-generated prompts, used to generate watermarked images via six methods: post-hoc (DwtDctSvd [12], RivaGAN [95], SSL [16], StegaStamp [81]) and in-generation (TreeRing [85], StableSignature [17]).

Baseline Methods We compare with three regeneration-based baselines: Regen [107] (100-step noise injection), Rinse-2xDiff [1], and CtrlRegen [46], with Stable Diffusion-v1.5 as the base model.

Evaluation Metrics The efficacy of watermark removal is evaluated using two core metrics: average Bit Accuracy (BitAcc) and TPR@1%FPR (True Positive Rate at 1% False Positive Rate). BitAcc quantifies correctly recovered bits in

multi-bit watermarking, with lower values meaning more thorough watermark destruction. TPR@1%FPR assesses removal stealth by calculating true positive rate under 1% false positive rate, where smaller values indicate harder-to-detect effects. For clarity, both metrics are reported for watermarked images before (BitAcc B, TPR@1%FPR B) and after (BitAcc A, TPR@1%FPR A) attack.

In terms of image quality assessment, metrics include Peak Signal-to-Noise Ratio (PSNR) and Structural Similarity Index (SSIM), which evaluate at the pixel level. Additionally, we also adopt Learned Perceptual Image Patch Similarity (LPIPS) [97], Deep Image Structure and Texture Similarity (DISTS) [14], Quality-Align (Q-Align) [86], CLIP-based Image Quality Assessment (CLIP-IQA) [83], and Fréchet Inception Distance (FID) [28] as evaluation metrics, which can measure the similarity and quality differences between images from the perspective of human visual perception.

4.2. Comparison and Evaluation

Quantitative Evaluation Figure 2 presents a comparative analysis of TokenPure against three alternative methods under varying noise intensities, evaluated across four low-perturbation watermarking schemes (DwtDctSvd, RivaGAN, SSL, and StableSignature) and two high-perturbation counterparts (StegaStamp and TreeRing). For low-perturbation watermarks, the number of noising steps was set to {50, 100, 150, 200, 300}. Compared to Regen and Rinse, TokenPure not only maintains superior image quality and similarity but also achieves state-of-the-art watermark removal performance. Specifically, under the same TPR@1%FPR criterion, our method outperforms competing approaches in both pixel-level metrics (PSNR/SSIM) and perceptual quality assessments (Q-Align/FID).

For high-perturbation watermarks, the noising steps were extended to {100, 200, 300, 400, 500}. While Regen and Rinse can achieve watermark removal with excessive noise injection, they cause substantial degradation to the original image content. Notably, when the number of noising steps exceeds 500, the regenerated images lose critical original information, rendering the watermark removal process meaningless. Although CtrlRegen can disrupt high-perturbation watermarks while preserving basic image content, it suffers from significant deviations in semantic information. In contrast, TokenPure achieves effective watermark removal while retaining the integrity of the original image information, striking a better balance between watermark erasure efficacy and image consistency. Additional quantitative results across other evaluation metrics are provided in the supplementary materials.

Qualitative Evaluation Figure 3 shows visual comparisons of watermark removal attacks across methods, with each watermarking column including an attacked image and a

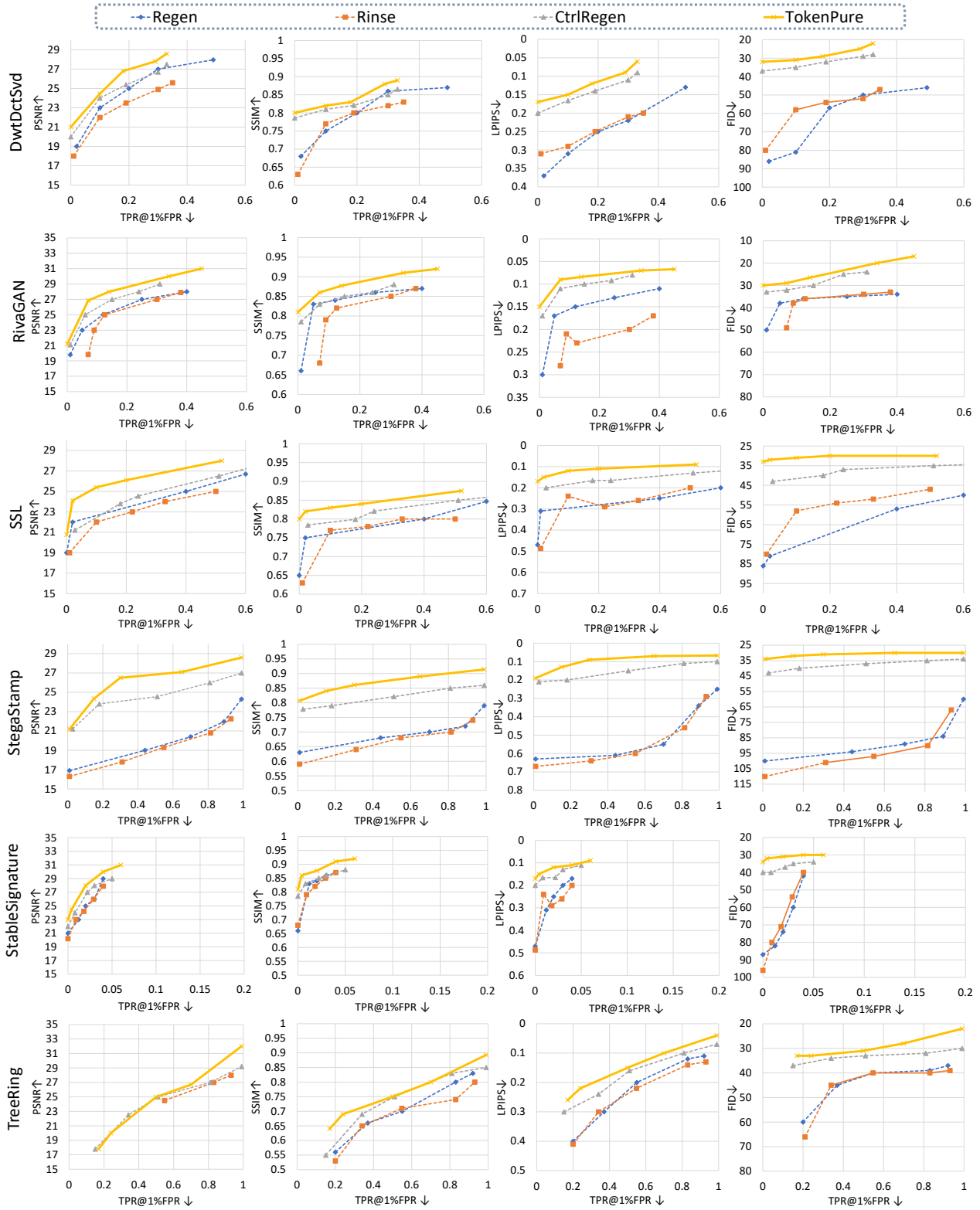


Figure 2. Performance of TokenPure compared to other methods with a varying number of noise strengths on different watermarks, respectively. We invert the LPIPS/FID scores to ensure that the top-left represents better performance across all figures.

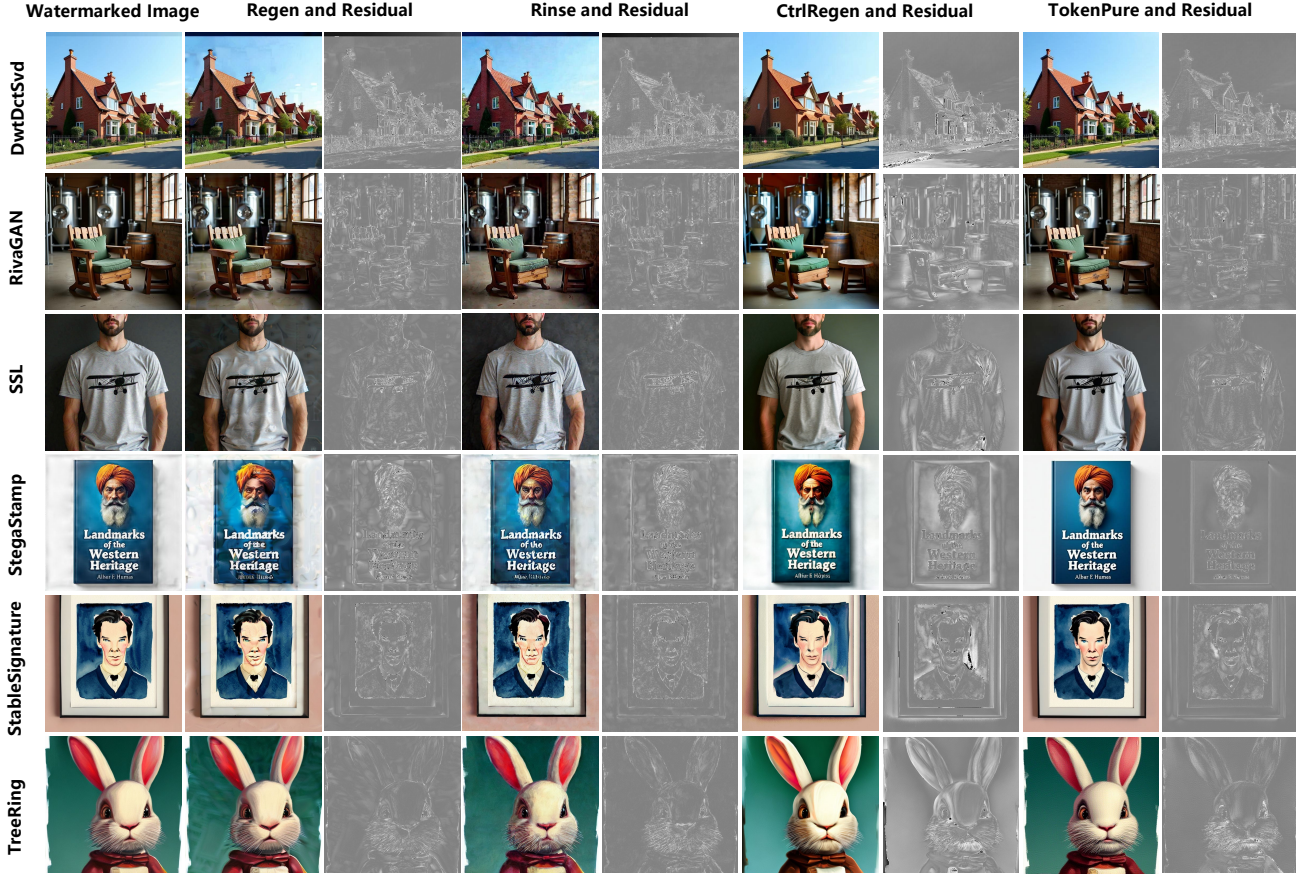


Figure 3. Qualitative comparison of different watermark removal attacks on different watermarking methods. It shows that our TokenPure preserves high visual consistency and quality under various watermarks.

residual map (difference between attacked and original un-watermarked images). In low-perturbation scenarios, TokenPure’s generated images are highly consistent with originals in texture and color. For RivaGAN, furniture details in TokenPure’s result fully match the original, while Regen, Rinse, and CtrlRegen show obvious local deviations in color and texture. For high-perturbation watermarks, TokenPure removes watermarks while preserving original core features. Regen and Rinse leave background artifacts due to

watermark noise. Though CtrlRegen avoids noise influence for a clean background, it has slight style deviations. In contrast, TokenPure’s images are nearly identical to originals in color saturation.

Furthermore, we conduct a dedicated study on inference efficiency (detailed in the supplementary materials) to provide a practical efficiency-performance trade-off. Additionally, we supplement more visual results for related experiments to enhance result interpretability.

4.3. Model Analysis

In this section, we conduct an ablation study on the effectiveness of our proposed method.

Ablation study We compared three pipelines in watermark removal, including directly inputting the original image as a visual prompt, using the semantic token prompt, and combining semantic tokens with edge control. As shown in Table 1, in terms of both bit accuracy destruction and the stealth of watermark removal, the token compression-based methods significantly outperform simple image resizing control. This indicates that the semantic

Table 1. Performance comparison of visual token compression for Watermark removal. Results show that visual tokens achieve superior watermark weakening capability.

Watermarks	method	BitAcc B \uparrow	BitAcc A \downarrow	TPR@1% FPR B \uparrow	TPR A \downarrow FPR A \downarrow
StegaStamp	Resize image control	1.0	0.6584	1.0	0.5420
	semantic token	1.0	0.4821	1.0	0.0025
	semantic token & canny control	1.0	0.4947	1.0	0.0080
TreeRing	Resize image control	1.0	0.8268	1.0	0.4087
	semantic token	1.0	0.7524	1.0	0.1270
	semantic token & canny control	1.0	0.7670	1.0	0.1580

Table 2. Ablation study on the effectiveness of the Layout Controller (LC), Appearance Adapter (AA), and Joint Consistency Reward (JCR) mechanism in image reconstruction. The best results are denoted as **bold**. The results reveal that AA and LC considerably improve the image quality, while the JCR mechanism further enhances image consistency.

Model	AA	Redux	LC	JCR	PSNR (dB) ↑	SSIM ↑	LPIPS ↓	DISTS ↓	Q-Align ↑	CLIP-IQA ↑	FID ↓
A	✓				15.89	0.6354	0.4483	0.2757	3.609	0.7379	79.59
B		✓			13.85	0.5858	0.5053	0.2955	3.629	0.7249	85.58
C		✓	✓		17.44	0.6713	0.2986	0.2004	4.012	0.7641	56.85
D	✓		✓		20.29	0.7937	0.2088	0.1395	4.092	0.7689	35.30
E	✓		✓	✓	21.19	0.8074	0.1920	0.1347	4.197	0.7743	33.34

Table 3. Evaluation of watermarking methods against VAE reconstruction. It is proven that different watermarks exhibit strong robustness to VAE.

Watermarks	BitAcc B ↑	BitAcc A ↓	TPR@1%FPR B ↑	TPR@1%FPR A ↓
SSL	1.0	0.8872	1.0	0.8250
StegaStamp	1.0	0.9991	1.0	1.000
TreeRing	1.0	1.000	1.0	1.000

guidance strategy based on token compression can effectively destroy the bit structure of watermarks and reduce their recognizability. Particularly, the experimental results on two types of watermarks with strong perturbations further verify the universal effectiveness of token compression in watermark removal tasks.

We also conduct an ablation study to verify the effectiveness of TokenPure’s modules (see in Table 2), confirming each module’s necessity and synergistic effect. To validate the Appearance Adapter (AA), we use FLUX.1 Redux, a prompt-based reconstruction adapter, as a baseline.

Through comparison, it is found that the core metrics of Model A/D (with AA) are comprehensively superior to those of Model B/C (with Redux). This indicates that when processing visual tokens, AA can more accurately preserve details such as color and texture, whereas Redux tends to focus on style transfer with weaker guidance from semantic information. For the Layout Controller (LC), horizontal comparison between Model A/B (without LC) and Model C/D (with LC) shows that with the same semantic adapter, all metrics are significantly optimized after adding LC. This proves that LC can effectively address the problem of spatial layout blurriness and enhance the structural integrity of images. Furthermore, comparing Model D and E reveals that all metrics are improved after integrating the Joint Consistency Reward (JCR), especially indicators like PSNR. This demonstrates that the pixel-level consistency constraint of JCR can further reduce reconstruction errors on the basis of the dual-branch architecture, enhancing the visual consistency between the reconstructed image and the original image, and ultimately achieving state-of-the-art performance.

To further demonstrate our method’s effectiveness, we tested VAE-based watermark attacks. Table 3 shows that after VAE reconstruction, all three watermarking methods re-

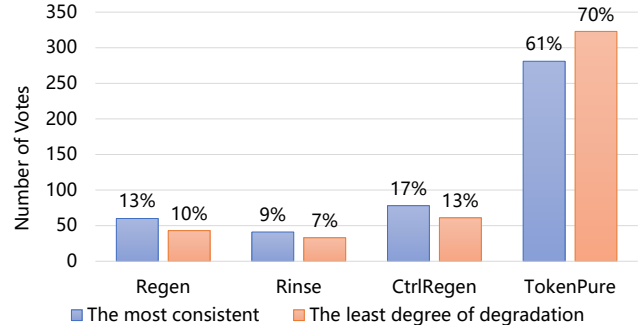


Figure 4. User study results. Our TokenPure is preferred by human voters over other baselines. The results show the advantages of Tokenpure in both image consistency and degradation control.

tain high bit accuracy and detectability (close to 1), indicating strong robustness to VAE reconstruction and that VAE alone cannot effectively destroy or remove watermarks. We also provide a more efficient version and additional visual comparison results in the supplementary materials.

4.4. User Study

For comprehensive watermark removal evaluation, we conducted a user study comparing TokenPure with baselines (Regen, Rinse, CtrlRegen). 46 voters assessed 10 image groups (each with 4 removal results and 1 unwatermarked reference), answering two questions: 1) select the result most consistent with the reference, and 2) select the one with the least degradation/artifacts. As shown in Figure 4, TokenPure led the 920 total votes (46×10×2), winning 61% for “most consistent” and 70% for “least degradation”—far exceeding others. This confirms its superiority in both reference consistency and perceptual quality.

5. Conclusion

In this paper, we introduced TokenPure, a novel dual-branch Diffusion Transformer framework specifically engineered for the watermark removal task. By integrating an Appearance Adapter and a Layout Controller, it effectively addresses the critical challenge of removing watermarks while safeguarding both the quality and structural consistency of

the original image. Extensive experimental results demonstrate that TokenPure achieves state-of-the-art performance across comprehensive benchmarks, successfully overcoming the limitations of traditional methods in handling high-perturbation watermarks, which solidifies its standing as a robust solution for watermark removal research.

References

- [1] Bang An, Mucong Ding, Tahseen Rabbani, Aakriti Agrawal, Yuancheng Xu, Chenghao Deng, Sicheng Zhu, Abdirisak Mohamed, Yuxin Wen, Tom Goldstein, et al. Benchmarking the robustness of image watermarks. *arXiv preprint arXiv:2401.08573*, 2024. 1, 5
- [2] Li An, Yujian Liu, Yepeng Liu, Yuheng Bu, Yang Zhang, and Shiyu Chang. A reinforcement learning framework for robust and secure llm watermarking. *arXiv preprint arXiv:2510.21053*, 2025. 1
- [3] Li An, Yujian Liu, Yepeng Liu, Yang Zhang, Yuheng Bu, and Shiyu Chang. Defending llm watermarking against spoofing attacks with contrastive representation learning. *arXiv preprint arXiv:2504.06575*, 2025. 1
- [4] Kasra Arabi, R Teal Witter, Chinmay Hegde, and Niv Cohen. Seal: Semantic aware image watermarking. In *Proceedings of the IEEE/CVF International Conference on Computer Vision*, pages 16196–16205, 2025. 2
- [5] Tim Brooks, Aleksander Holynski, and Alexei A Efros. Instructpix2pix: Learning to follow image editing instructions. In *Proceedings of the IEEE/CVF Conference on Computer Vision and Pattern Recognition*, pages 18392–18402, 2023. 2
- [6] Soravit Changpinyo, Piyush Sharma, Nan Ding, and Radu Soricut. Conceptual 12M: Pushing web-scale image-text pre-training to recognize long-tail visual concepts. In *CVPR*, 2021. 5
- [7] Huili Chen, Bitu Darvish Rouhani, Cheng Fu, Jishen Zhao, and Farinaz Koushanfar. Deepmarks: A secure fingerprinting framework for digital rights management of deep learning models. In *Proceedings of the 2019 International Conference on Multimedia Retrieval*, pages 105–113, 2019. 2
- [8] Ruibo Chen, Sheng Zhang, Yihan Wu, Tong Zheng, Peihua Mai, and Heng Huang. Model correlation detection via random selection probing. *arXiv preprint arXiv:2509.24171*, 2025. 1
- [9] Xuewei Chen, Zhimin Chen, and Yiren Song. Transanimate: Taming layer diffusion to generate rgba video. *arXiv preprint arXiv:2503.17934*, 2025. 2
- [10] Hai Ci, Yiren Song, Pei Yang, Jinheng Xie, and Mike Zheng Shou. Wmadapter: Adding watermark control to latent diffusion models. *arXiv preprint arXiv:2406.08337*, 2024. 1, 2
- [11] Hai Ci, Pei Yang, Yiren Song, and Mike Zheng Shou. Ringid: Rethinking tree-ring watermarking for enhanced multi-key identification. *arXiv preprint arXiv:2404.14055*, 2024. 1, 2
- [12] Ingemar Cox, Matthew Miller, Jeffrey Bloom, Jessica Fridrich, and Ton Kalker. *Digital watermarking and steganography*. Morgan kaufmann, 2007. 1, 2, 5
- [13] Jia Deng, Wei Dong, Richard Socher, Li-Jia Li, Kai Li, and Li Fei-Fei. Imagenet: A large-scale hierarchical image database. In *2009 IEEE Conference on Computer Vision and Pattern Recognition*, pages 248–255. IEEE, 2009. 5
- [14] Keyan Ding, Kede Ma, Shiqi Wang, and Eero P Simoncelli. Image quality assessment: Unifying structure and texture similarity. *IEEE transactions on pattern analysis and machine intelligence*, 44(5):2567–2581, 2020. 5
- [15] Ben Egan, Alex Redden, XWAVE, and SilentAntagonist. Dalle3 1 Million+ High Quality Captions, 2024. 5
- [16] Pierre Fernandez, Alexandre Sablayrolles, Teddy Furon, Hervé Jégou, and Matthijs Douze. Watermarking images in self-supervised latent spaces. In *ICASSP 2022-2022 IEEE International Conference on Acoustics, Speech and Signal Processing (ICASSP)*, pages 3054–3058. IEEE, 2022. 1, 2, 5
- [17] Pierre Fernandez, Guillaume Couairon, Hervé Jégou, Matthijs Douze, and Teddy Furon. The stable signature: Rooting watermarks in latent diffusion models. *ICCV*, 2023. 1, 2, 5
- [18] Rinon Gal, Yuval Alaluf, Yuval Atzmon, Or Patashnik, Amit H Bermano, Gal Chechik, and Daniel Cohen-Or. An image is worth one word: Personalizing text-to-image generation using textual inversion. *arXiv preprint arXiv:2208.01618*, 2022. 3
- [19] Yan Gong, Yiren Song, Yicheng Li, Chenglin Li, and Yin Zhang. Relationadapter: Learning and transferring visual relation with diffusion transformers. *arXiv preprint arXiv:2506.02528*, 2025. 3
- [20] Zixuan Gong, Guangyin Bao, Qi Zhang, Zhongwei Wan, Duoqian Miao, Shoujin Wang, Lei Zhu, Changwei Wang, Rongtao Xu, Liang Hu, et al. Neuroclips: Towards high-fidelity and smooth fmri-to-video reconstruction. *Advances in Neural Information Processing Systems*, 37: 51655–51683, 2024. 1
- [21] Sam Gunn, Xuandong Zhao, and Dawn Song. An undetectable watermark for generative image models. *arXiv preprint arXiv:2410.07369*, 2024. 1
- [22] Hailong Guo, Bohan Zeng, Yiren Song, Wentao Zhang, Chuang Zhang, and Jiaming Liu. Any2anytryon: Leveraging adaptive position embeddings for versatile virtual clothing tasks. *arXiv preprint arXiv:2501.15891*, 2025. 3
- [23] Junfeng Guo, Yiming Li, Ruibo Chen, Yihan Wu, Heng Huang, et al. Zeromark: Towards dataset ownership verification without disclosing watermark. *Advances in Neural Information Processing Systems*, 37:120468–120500, 2024. 1
- [24] Haiyun He, Yepeng Liu, Ziqiao Wang, Yongyi Mao, and Yuheng Bu. Universally optimal watermarking schemes for llms: from theory to practice. *arXiv preprint arXiv:2410.02890*, 2024. 1
- [25] Haiyun He, Yepeng Liu, Ziqiao Wang, Yongyi Mao, and Yuheng Bu. Distributional information embedding: A framework for multi-bit watermarking. *arXiv preprint arXiv:2501.16558*, 2025. 1

- [26] D Hendrycks. Gaussian error linear units (gelus). *arXiv preprint arXiv:1606.08415*, 2016. 5
- [27] Amir Hertz, Ron Mokady, Jay Tenenbaum, Kfir Aberman, Yael Pritch, and Daniel Cohen-Or. Prompt-to-prompt image editing with cross attention control. *arXiv preprint arXiv:2208.01626*, 2022. 2
- [28] Martin Heusel, Hubert Ramsauer, Thomas Unterthiner, Bernhard Nessler, and Sepp Hochreiter. Gans trained by a two time-scale update rule converge to a local nash equilibrium. *Advances in neural information processing systems*, 30, 2017. 5
- [29] Jonathan Ho, Ajay Jain, and Pieter Abbeel. Denoising diffusion probabilistic models. *Advances in neural information processing systems*, 33:6840–6851, 2020. 2
- [30] Edward J Hu, Yelong Shen, Phillip Wallis, Zeyuan Allen-Zhu, Yuanzhi Li, Shean Wang, Lu Wang, and Weizhu Chen. LoRA: Low-rank adaptation of large language models. In *International Conference on Learning Representations*, 2022. 3, 4
- [31] Yuepeng Hu, Zhengyuan Jiang, Moyang Guo, and Neil Gong. A transfer attack to image watermarks. *arXiv preprint arXiv:2403.15365*, 2024. 2
- [32] Shijie Huang, Yiren Song, Yuxuan Zhang, Hailong Guo, Xueyin Wang, and Jiaming Liu. Arteditor: Learning customized instructional image editor from few-shot examples. In *Proceedings of the IEEE/CVF International Conference on Computer Vision*, pages 17651–17662, 2025. 3
- [33] Siqui Hui, Yiren Song, Sanping Zhou, Ye Deng, Wenli Huang, and Jinjun Wang. Autoregressive images watermarking through lexical biasing: An approach resistant to regeneration attack. *arXiv preprint arXiv:2506.01011*, 2025. 1
- [34] Hengrui Jia, Christopher A Choquette-Choo, Varun Chandrasekaran, and Nicolas Papernot. Entangled watermarks as a defense against model extraction. In *30th USENIX security symposium (USENIX Security 21)*, pages 1937–1954, 2021. 2
- [35] Yuxin Jiang, Yuchao Gu, Yiren Song, Ivor Tsang, and Mike Zheng Shou. Personalized vision via visual in-context learning. *arXiv preprint arXiv:2509.25172*, 2025. 3
- [36] Zhengyuan Jiang, Jinghuai Zhang, and Neil Zhenqiang Gong. Evading watermark based detection of ai-generated content. In *Proceedings of the 2023 ACM SIGSAC Conference on Computer and Communications Security*, pages 1168–1181, 2023. 2
- [37] Andre Kassis and Urs Hengartner. Unmarker: A universal attack on defensive watermarking. *arXiv preprint arXiv:2405.08363*, 2024. 2
- [38] Nupur Kumari, Bingliang Zhang, Richard Zhang, Eli Shechtman, and Jun-Yan Zhu. Multi-concept customization of text-to-image diffusion. In *Proceedings of the IEEE/CVF Conference on Computer Vision and Pattern Recognition*, pages 1931–1941, 2023. 3
- [39] Black Forest Labs. Flux. <https://github.com/black-forest-labs/flux>, 2024. 5
- [40] Sung Ju Lee and Nam Ik Cho. Semantic watermarking reinvented: Enhancing robustness and generation quality with fourier integrity. In *Proceedings of the IEEE/CVF International Conference on Computer Vision*, pages 18759–18769, 2025. 2
- [41] Ming Li, Taojiannan Yang, Huafeng Kuang, Jie Wu, Zhaoning Wang, Xuefeng Xiao, and Chen Chen. Controlnet++: Improving conditional controls with efficient consistency feedback: Project page: liming-ai. github.io/controlnet_plus_plus. In *European Conference on Computer Vision*, pages 129–147. Springer, 2024. 2
- [42] Jiacheng Liang, Zian Wang, Spencer Hong, Shouling Ji, and Ting Wang. Watermark under fire: A robustness evaluation of llm watermarking. In *Findings of the Association for Computational Linguistics: EMNLP 2025*, pages 21050–21074, 2025. 2
- [43] Aiwei Liu, Leyi Pan, Yijian Lu, Jingjing Li, Xuming Hu, Xi Zhang, Lijie Wen, Irwin King, Hui Xiong, and Philip Yu. A survey of text watermarking in the era of large language models. *ACM Computing Surveys*, 57(2):1–36, 2024. 1
- [44] Haotian Liu, Chunyuan Li, Qingyang Wu, and Yong Jae Lee. Visual instruction tuning. *Advances in neural information processing systems*, 36:34892–34916, 2023. 1
- [45] Yepeng Liu and Yuheng Bu. Adaptive text watermark for large language models. *arXiv preprint arXiv:2401.13927*, 2024. 1
- [46] Yepeng Liu, Yiren Song, Hai Ci, Yu Zhang, Haofan Wang, Mike Zheng Shou, and Yuheng Bu. Image watermarks are removable using controllable regeneration from clean noise. *arXiv preprint arXiv:2410.05470*, 2024. 1, 5
- [47] Yepeng Liu, Xuandong Zhao, Christopher Kruegel, Dawn Song, and Yuheng Bu. In-context watermarks for large language models. *arXiv preprint arXiv:2505.16934*, 2025. 1
- [48] Yepeng Liu, Xuandong Zhao, Dawn Song, and Yuheng Bu. Dataset protection via watermarked canaries in retrieval-augmented llms. *arXiv preprint arXiv:2502.10673*, 2025. 1
- [49] Yepeng Liu, Xuandong Zhao, Dawn Song, Gregory W Wornell, and Yuheng Bu. Position: Llm watermarking should align stakeholders’ incentives for practical adoption. *arXiv preprint arXiv:2510.18333*, 2025. 1
- [50] Ilya Loshchilov and Frank Hutter. Decoupled weight decay regularization. *arXiv preprint arXiv:1711.05101*, 2017. 5
- [51] Runnan Lu, Yuxuan Zhang, Jiaming Liu, Haofan Wang, and Yiren Song. Easytext: Controllable diffusion transformer for multilingual text rendering. *arXiv preprint arXiv:2505.24417*, 2025. 3
- [52] Nils Lukas, Abdulrahman Diaa, Lucas Fenaux, and Florian Kerschbaum. Leveraging optimization for adaptive attacks on image watermarks. *arXiv preprint arXiv:2309.16952*, 2023. 2
- [53] Ziyuan Luo, Yangyi Zhao, Ka Chun Cheung, Simon See, and Renjie Wan. Imagesentinel: Protecting visual datasets from unauthorized retrieval-augmented image generation. *arXiv preprint arXiv:2510.12119*, 2025. 1
- [54] Yue Ma, Xiaodong Cun, Yingqing He, Chenyang Qi, Xintao Wang, Ying Shan, Xiu Li, and Qifeng Chen. Magicstick: Controllable video editing via control handle transformations. *arXiv preprint arXiv:2312.03047*, 2023. 2

- [55] Yue Ma, Yingqing He, Xiaodong Cun, Xintao Wang, Siran Chen, Xiu Li, and Qifeng Chen. Follow your pose: Pose-guided text-to-video generation using pose-free videos. In *Proceedings of the AAAI Conference on Artificial Intelligence*, pages 4117–4125, 2024.
- [56] Yue Ma, Hongyu Liu, Hongfa Wang, Heng Pan, Yingqing He, Junkun Yuan, Ailing Zeng, Chengfei Cai, Heung-Yeung Shum, Wei Liu, et al. Follow-your-emoji: Fine-controllable and expressive freestyle portrait animation. In *SIGGRAPH Asia 2024 Conference Papers*, pages 1–12, 2024.
- [57] Yue Ma, Kunyu Feng, Xinhua Zhang, Hongyu Liu, David Junhao Zhang, Jinbo Xing, Yinhan Zhang, Ayden Yang, Zeyu Wang, and Qifeng Chen. Follow-your-creation: Empowering 4d creation through video inpainting. *arXiv preprint arXiv:2506.04590*, 2025.
- [58] Yue Ma, Yingqing He, Hongfa Wang, Andong Wang, Leqi Shen, Chenyang Qi, Jixuan Ying, Chengfei Cai, Zhifeng Li, Heung-Yeung Shum, et al. Follow-your-click: Open-domain regional image animation via motion prompts. In *Proceedings of the AAAI Conference on Artificial Intelligence*, pages 6018–6026, 2025.
- [59] Yue Ma, Yulong Liu, Qiyuan Zhu, Ayden Yang, Kunyu Feng, Xinhua Zhang, Zhifeng Li, Sirui Han, Chenyang Qi, and Qifeng Chen. Follow-your-motion: Video motion transfer via efficient spatial-temporal decoupled finetuning. *arXiv preprint arXiv:2506.05207*, 2025. 2
- [60] Po-Yuan Mao, Cheng-Chang Tsai, and Chun-Shien Lu. Maxsive: High-capacity and robust training-free generative image watermarking in diffusion models. In *Proceedings of the 33rd ACM International Conference on Multimedia*, pages 11443–11452, 2025. 2
- [61] Chong Mou, Xintao Wang, Liangbin Xie, Jian Zhang, Zhongang Qi, Ying Shan, and Xiaohu Qie. T2i-adapter: Learning adapters to dig out more controllable ability for text-to-image diffusion models. *arXiv preprint arXiv:2302.08453*, 2023. 2
- [62] Andreas Müller, Denis Lukovnikov, Jonas Thietke, Asja Fischer, and Erwin Quiring. Black-box forgery attacks on semantic watermarks for diffusion models. In *Proceedings of the Computer Vision and Pattern Recognition Conference*, pages 20937–20946, 2025. 2
- [63] William Peebles and Saining Xie. Scalable diffusion models with transformers. In *Proceedings of the IEEE/CVF International Conference on Computer Vision*, pages 4195–4205, 2023. 2, 3
- [64] Ben Poole, Ajay Jain, Jonathan T Barron, and Ben Mildenhall. Dreamfusion: Text-to-3d using 2d diffusion. *arXiv preprint arXiv:2209.14988*, 2022. 2
- [65] Alec Radford, Jong Wook Kim, Chris Hallacy, Aditya Ramesh, Gabriel Goh, Sandhini Agarwal, Girish Sastry, Amanda Askell, Pamela Mishkin, Jack Clark, et al. Learning transferable visual models from natural language supervision. In *International conference on machine learning*, pages 8748–8763. PmlR, 2021. 2
- [66] Colin Raffel, Noam Shazeer, Adam Roberts, Katherine Lee, Sharan Narang, Michael Matena, Yanqi Zhou, Wei Li, and Peter J. Liu. Exploring the limits of transfer learning with a unified text-to-text transformer. *Journal of Machine Learning Research*, 21(140):1–67, 2020. 3
- [67] Robin Rombach, Andreas Blattmann, Dominik Lorenz, Patrick Esser, and Björn Ommer. High-resolution image synthesis with latent diffusion models. In *Proceedings of the IEEE/CVF conference on computer vision and pattern recognition*, pages 10684–10695, 2022. 1, 2
- [68] Bitu Darvish Rouhani, Huili Chen, and Farinaz Koushanfar. Deepsigns: A generic watermarking framework for ip protection of deep learning models. *arXiv preprint arXiv:1804.00750*, 2018. 2
- [69] Nataniel Ruiz, Yuanzhen Li, Varun Jampani, Yael Pritch, Michael Rubinstein, and Kfir Aberman. Dreambooth: Fine tuning text-to-image diffusion models for subject-driven generation. 2022. 3
- [70] Mehrdad Saberi, Vinu Sankar Sadasivan, Keivan Rezaei, Aounon Kumar, Atoosa Chegini, Wenxiao Wang, and Soheil Feizi. Robustness of ai-image detectors: Fundamental limits and practical attacks. *arXiv preprint arXiv:2310.00076*, 2023. 1, 2
- [71] Hui Shen, Jingxuan Zhang, Boning Xiong, Rui Hu, Shoufa Chen, Zhongwei Wan, Xin Wang, Yu Zhang, Zixuan Gong, Guangyin Bao, et al. Efficient diffusion models: A survey. *arXiv preprint arXiv:2502.06805*, 2025. 1
- [72] Wenda Shi, Yiren Song, Dengming Zhang, Jiaming Liu, and Xingxing Zou. Fonts: Text rendering with typography and style controls. *arXiv preprint arXiv:2412.00136*, 2024. 3
- [73] Wenda Shi, Yiren Song, Zihan Rao, Dengming Zhang, Jiaming Liu, and Xingxing Zou. Wordcon: Word-level typography control in scene text rendering. *arXiv preprint arXiv:2506.21276*, 2025. 3
- [74] Jiaming Song, Chenlin Meng, and Stefano Ermon. Denoising diffusion implicit models. *arXiv preprint arXiv:2010.02502*, 2020. 2
- [75] Yiren Song, Shijie Huang, Chen Yao, Xiaojun Ye, Hai Ci, Jiaming Liu, Yuxuan Zhang, and Mike Zheng Shou. Processpainter: Learn painting process from sequence data. *arXiv preprint arXiv:2406.06062*, 2024. 2
- [76] Yiren Song, Shengtao Lou, Xiaokang Liu, Hai Ci, Pei Yang, Jiaming Liu, and Mike Zheng Shou. Anti-reference: Universal and immediate defense against reference-based generation. *arXiv preprint arXiv:2412.05980*, 2024. 1
- [77] Yiren Song, Danze Chen, and Mike Zheng Shou. Layer-tracer: Cognitive-aligned layered svg synthesis via diffusion transformer. *arXiv preprint arXiv:2502.01105*, 2025. 3
- [78] Yiren Song, Cheng Liu, and Mike Zheng Shou. Makeanything: Harnessing diffusion transformers for multi-domain procedural sequence generation. *arXiv preprint arXiv:2502.01572*, 2025.
- [79] Yiren Song, Cheng Liu, and Mike Zheng Shou. Omniconsistency: Learning style-agnostic consistency from paired stylization data. *arXiv preprint arXiv:2505.18445*, 2025. 3
- [80] Yiren Song, Pei Yang, Hai Ci, and Mike Zheng Shou. Id-protector: An adversarial noise encoder to protect against

- id-preserving image generation. In *Proceedings of the Computer Vision and Pattern Recognition Conference*, pages 3019–3028, 2025. 1
- [81] Matthew Tancik, Ben Mildenhall, and Ren Ng. Stegas-tamp: Invisible hyperlinks in physical photographs. In *IEEE Conference on Computer Vision and Pattern Recognition (CVPR)*, 2020. 1, 2, 5
- [82] Cong Wan, Xiangyang Luo, Zijian Cai, Yiren Song, Yunlong Zhao, Yifan Bai, Yuhang He, and Yihong Gong. Grid: Visual layout generation. *arXiv preprint arXiv:2412.10718*, 2024. 3
- [83] Jianyi Wang, Kelvin CK Chan, and Chen Change Loy. Exploring clip for assessing the look and feel of images. In *AAAI*, 2023. 5
- [84] Zitong Wang, Hang Zhao, Qianyu Zhou, Xuequan Lu, Xiangtai Li, and Yiren Song. Diffdecompose: Layer-wise decomposition of alpha-composited images via diffusion transformers. *arXiv preprint arXiv:2505.21541*, 2025. 3
- [85] Yuxin Wen, John Kirchenbauer, Jonas Geiping, and Tom Goldstein. Tree-rings watermarks: Invisible fingerprints for diffusion images. *Advances in Neural Information Processing Systems*, 36, 2024. 1, 2, 5
- [86] Haoning Wu, Zicheng Zhang, Weixia Zhang, Chaofeng Chen, Chunyi Li, Liang Liao, Annan Wang, Erli Zhang, Wenxiu Sun, Qiong Yan, Xionguo Min, Guangtai Zhai, and Weisi Lin. Q-align: Teaching Imms for visual scoring via discrete text-defined levels. *arXiv preprint arXiv:2312.17090*, 2023. 5
- [87] Yihan Wu, Xuehao Cui, Ruiibo Chen, Georgios Milis, and Heng Huang. A watermark for auto-regressive image generation models. *arXiv preprint arXiv:2506.11371*, 2025. 2
- [88] Yihan Wu, Georgios Milis, Ruiibo Chen, and Heng Huang. Robust distortion-free watermark for autoregressive audio generation models. *arXiv preprint arXiv:2510.21115*, 2025. 1
- [89] Pei Yang, Hai Ci, Yiren Song, and Mike Zheng Shou. Can simple averaging defeat modern watermarks? *Advances in Neural Information Processing Systems*, 37:56644–56673, 2024. 2
- [90] Zijin Yang, Kai Zeng, Kejiang Chen, Han Fang, Weiming Zhang, and Nenghai Yu. Gaussian shading: Provable performance-lossless image watermarking for diffusion models. In *Proceedings of the IEEE/CVF Conference on Computer Vision and Pattern Recognition*, pages 12162–12171, 2024. 1
- [91] Hu Ye, Jun Zhang, Sibao Liu, Xiao Han, and Wei Yang. Ip-adapt: Text compatible image prompt adapter for text-to-image diffusion models. *arXiv preprint arXiv:2308.06721*, 2023. 3
- [92] Junyan Ye, Dongzhi Jiang, Zihao Wang, Leqi Zhu, Zhenghao Hu, Zilong Huang, Jun He, Zhiyuan Yan, Jinghua Yu, Hongsheng Li, et al. Echo-4o: Harnessing the power of gpt-4o synthetic images for improved image generation. *arXiv preprint arXiv:2508.09987*, 2025. 5
- [93] Xiaohua Zhai, Basil Mustafa, Alexander Kolesnikov, and Lucas Beyer. Sigmoid loss for language image pre-training. In *Proceedings of the IEEE/CVF international conference on computer vision*, pages 11975–11986, 2023. 2, 3
- [94] Jingqi Zhang, Ruiibo Chen, Yingqing Yang, Peihua Mai, Heng Huang, and Yan Pang. Leave no trace: Black-box detection of copyrighted dataset usage in large language models via watermarking. *arXiv preprint arXiv:2510.02962*, 2025. 1
- [95] Kevin Alex Zhang, Lei Xu, Alfredo Cuesta-Infante, and Kalyan Veeramachaneni. Robust invisible video watermarking with attention. *arXiv preprint arXiv:1909.01285*, 2019. 1, 5
- [96] Lvmin Zhang and Maneesh Agrawala. Adding conditional control to text-to-image diffusion models. *arXiv preprint arXiv:2302.05543*, 2023. 2
- [97] Richard Zhang, Phillip Isola, Alexei A Efros, Eli Shechtman, and Oliver Wang. The unreasonable effectiveness of deep features as a perceptual metric. In *Proceedings of the IEEE conference on computer vision and pattern recognition*, pages 586–595, 2018. 5
- [98] Yu Zhang, Yepeng Liu, Duoqian Miao, Qi Zhang, Yiwei Shi, and Liang Hu. Mg-vit: a multi-granularity method for compact and efficient vision transformers. *Advances in Neural Information Processing Systems*, 36:69328–69347, 2023. 1
- [99] Yuxuan Zhang, Yiren Song, Jiaming Liu, Rui Wang, Jinpeng Yu, Hao Tang, Huaxia Li, Xu Tang, Yao Hu, Han Pan, et al. Ssr-encoder: Encoding selective subject representation for subject-driven generation. In *Proceedings of the IEEE/CVF Conference on Computer Vision and Pattern Recognition*, pages 8069–8078, 2024. 3
- [100] Yuxuan Zhang, Yiren Song, Jinpeng Yu, Han Pan, and Zhongliang Jing. Fast personalized text to image synthesis with attention injection. In *ICASSP 2024-2024 IEEE International Conference on Acoustics, Speech and Signal Processing (ICASSP)*, pages 6195–6199. IEEE, 2024. 3
- [101] Yuxuan Zhang, Lifu Wei, Qing Zhang, Yiren Song, Jiaming Liu, Huaxia Li, Xu Tang, Yao Hu, and Haibo Zhao. Stablemakeup: When real-world makeup transfer meets diffusion model. *arXiv preprint arXiv:2403.07764*, 2024. 2
- [102] Yu Zhang, Qi Zhang, Zixuan Gong, Yiwei Shi, Yepeng Liu, Duoqian Miao, Yang Liu, Ke Liu, Kun Yi, Wei Fan, et al. Mlip: Efficient multi-perspective language-image pretraining with exhaustive data utilization. *arXiv preprint arXiv:2406.01460*, 2024. 1
- [103] Yuxuan Zhang, Qing Zhang, Yiren Song, and Jiaming Liu. Stable-hair: Real-world hair transfer via diffusion model. *arXiv preprint arXiv:2407.14078*, 2024. 2
- [104] Yuxuan Zhang, Yirui Yuan, Yiren Song, Haofan Wang, and Jiaming Liu. Easycontrol: Adding efficient and flexible control for diffusion transformer. *arXiv preprint arXiv:2503.07027*, 2025. 3
- [105] Yu Zhang, Jialei Zhou, Xinchun Li, Qi Zhang, Zhongwei Wan, Duoqian Miao, Changwei Wang, and Longbing Cao. Enhancing text-to-image diffusion transformer via split-text conditioning. In *The Thirty-ninth Annual Conference on Neural Information Processing Systems*, 2025. 1
- [106] Xuandong Zhao, Sam Gunn, Miranda Christ, Jaiden Fairuze, Andres Fabrega, Nicholas Carlini, Sanjam Garg, Sanghyun Hong, Milad Nasr, Florian Tramer, et al.

Sok: Watermarking for ai-generated content, 2024. *URL* <https://arxiv.org/abs/2411.18479>. 1

- [107] Xuandong Zhao, Kexun Zhang, Zihao Su, Saastha Vasan, Ilya Grishchenko, Christopher Kruegel, Giovanni Vigna, Yu-Xiang Wang, and Lei Li. Invisible image watermarks are provably removable using generative ai. *arXiv preprint arXiv:2306.01953*, 2023. 1, 2, 5
- [108] J Zhu. Hidden: hiding data with deep networks. *arXiv preprint arXiv:1807.09937*, 2018. 1, 2
- [109] Zihang Zou, Boqing Gong, and Liqiang Wang. Attention to neural plagiarism: Diffusion models can plagiarize your copyrighted images! In *Proceedings of the IEEE/CVF International Conference on Computer Vision*, pages 19546–19556, 2025. 2

TokenPure: Watermark Removal through Tokenized Appearance and Structural Guidance

Supplementary Material

Details about Evaluation Metrics In terms of image quality assessment, metrics are categorized into two groups based on evaluation perspectives: Pixel-level metrics, including Peak Signal-to-Noise Ratio (PSNR) and Structural Similarity Index (SSIM). Peak Signal-to-Noise Ratio (PSNR) quantifies distortion mathematically by comparing signal strength to noise, with higher values indicating less distortion. Structural Similarity Index (SSIM) focuses on structural consistency across brightness, contrast, and spatial structure, with values closer to 1 reflecting stronger similarity to the original image at the pixel level.

Perceptual-level metrics, encompassing Learned Perceptual Image Patch Similarity (LPIPS), Deep Image Structure and Texture Similarity (DISTS), Quality-Align (Q-Align), CLIP-based Image Quality Assessment (CLIP-IQA), and Fréchet Inception Distance (FID). Both LPIPS and DISTS employ deep neural networks to quantify perceptual differences; consistently, lower metric values correspond to higher perceived similarity. DISTS is specifically designed to heighten sensitivity to structural and textural integrity, granting it greater tolerance for subtle color shifts. Q-Align integrates text-image alignment and visual quality, with higher scores denoting better alignment with textual instructions. CLIP-IQA, relying on cross-modal models, assesses quality or alignment without reference images, where higher values signal superior perceptual quality. FID measures the distance between feature distributions of generated and real images, with lower values indicating greater realism and diversity in generated content.

Running efficiency To assess TokenPure’s efficiency-performance trade-off, we analyze two key tables. Table 4 compares inference times across regeneration methods, while Table 5 evaluates TokenPure’s performance with different denoising timesteps. Table 4 reveals that TokenPure’s low-timestep variants (TokenPure-s4, TokenPure-s2) achieve substantial efficiency gains—with inference times reduced to 3.00s and 1.60s, respectively—compared to the full 25-timestep version (20.0s). Notably, these variants outpace competitors like Regen (0.60s, but with significant trade-offs in quality and removal efficacy) and CtrlRegen (2.56s, with semantic deviations). Table 5 further shows that fewer timesteps in TokenPure (e.g., s4, s2) introduce minor performance degradation in fine-grained detail reconstruction but retain core watermark removal capabilities. For instance, TokenPure-s4 maintains competitive BitAcc and TPR@1%FPR across all watermark types, while even

TokenPure-s2 outperforms the 25-timestep version in some metrics (e.g., BitAcc A for SSL). Although low-timestep variants lag slightly behind the full version in PSNR/SSIM, their efficiency improvement far outweighs the performance loss. Compared to existing methods, TokenPure’s low-timestep variants, despite marginally lower PSNR/SSIM than Regen, lead in watermark removal effectiveness, visual consistency, and inference efficiency. Thus, TokenPure-s4/s2 strike an optimal balance between efficiency and performance while preserving watermark removal advantages.

Table 4. Inference times of different regeneration methods.

Attack Methods	Number of steps	Times of Inferring(s)
Regen	60	0.60
Rinse	120	4.25
CtrlRegen	50	2.56
TokenPure	25	20.0
TokenPure-s4	4	3.00
TokenPure-s2	2	1.60

More Quantitative results Further comparisons across watermark types in another core metric, average Bit Accuracy (BitAcc) for watermark removal, confirm TokenPure’s advantages in removal effectiveness and image quality preservation. Figure 5 presents a comparative analysis of TokenPure against three alternative methods (Regen, Rinse, CtrlRegen) across six watermarking schemes (four low-perturbation ones: DwtDctSvd, RivaGAN, SSL, StableSignature; and two high-perturbation ones: StegaStamp, TreeRing). Unlike the metric TPR@1%FPR, the variation of BitAcc with different noise intensities is relatively subtle. However, from the overall trend, our method achieves higher image quality metrics such as PSNR, LPIPS, and FID under the same BitAcc. Taking the watermark StegaStamp as an example, when BitAcc is reduced to a comparable level, TokenPure maintains a PSNR that is 2–3 dB higher and an FID that is 15–20 points lower than Regen and Rinse, indicating significantly better structural and perceptual consistency.

It is evident that our method TokenPure achieves effective watermark removal (low BitAcc) while retaining original image integrity, striking a superior balance between erasure efficacy and consistency, where competing methods either fail to reduce BitAcc sufficiently or suffer from severe image degradation, whereas TokenPure consistently delivers both robust watermark erasure and high-fidelity reconstruction.

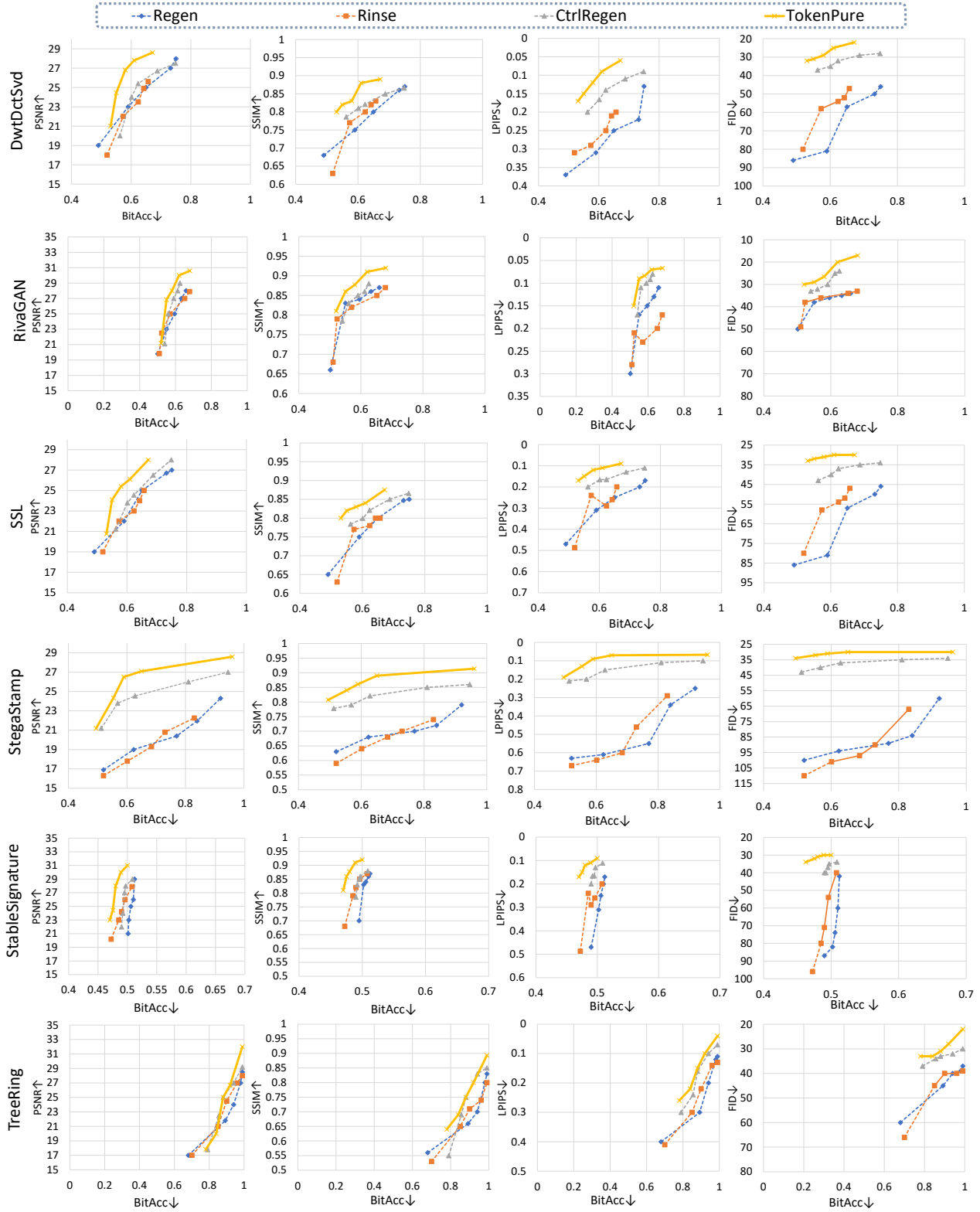


Figure 5. Performance of TokenPure compared to other methods with a varying number of noise strengths on different watermarks, respectively. We invert the LPIPS/FID scores to ensure that the top-left represents better performance across all figures.

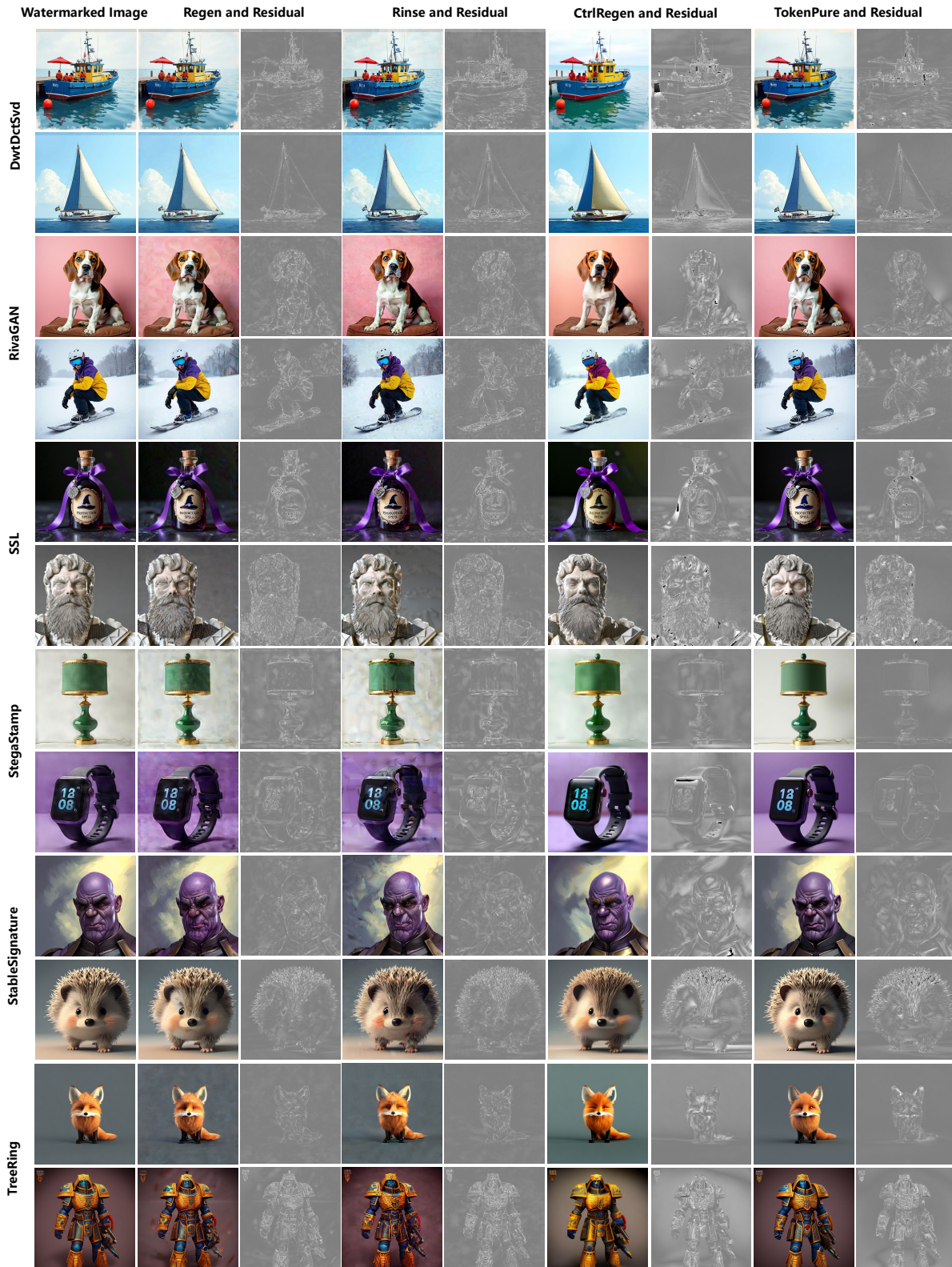


Figure 6. More qualitative comparison of different watermark removal attacks on different watermarking methods.

Table 5. Evaluation results of TokenPure with different denoising timesteps. The best results are denoted as **bold**.

Watermarks	Attack Methods	BitAcc B \uparrow	BitAcc A \downarrow	TPR@1%FPR B \uparrow	TPR@1%FPR A \downarrow	PSNR (dB) \uparrow	SSIM \uparrow	LPIPS \downarrow	DISTS \downarrow	Q-Align \uparrow	CLIP-IQA \uparrow	FID \downarrow
DwtDctSvd	TokenPure	0.9669	0.5001	0.9423	0.0000	19.77	0.7935	0.1832	0.1217	4.345	0.7859	32.95
	TokenPure-s4	0.9669	0.5021	0.9423	0.0000	19.18	0.7892	0.1981	0.1413	3.835	0.7825	37.46
	TokenPure-s2	0.9669	0.5009	0.9423	0.0000	19.64	0.7901	0.1940	0.1581	3.510	0.7742	44.59
RivaGAN	TokenPure	1.000	0.5270	1.000	0.0053	21.12	0.8056	0.1563	0.1098	4.415	0.7728	30.66
	TokenPure-s4	1.000	0.5446	1.000	0.0091	20.72	0.8053	0.1740	0.1348	3.869	0.7769	37.00
	TokenPure-s2	1.000	0.5826	1.000	0.0084	20.43	0.7976	0.1953	0.1593	3.484	0.7753	44.56
SSL	TokenPure	1.000	0.5314	1.000	0.0040	20.77	0.7954	0.1770	0.1363	4.476	0.7733	33.05
	TokenPure-s4	1.000	0.5094	1.000	0.0000	20.27	0.7948	0.1931	0.1557	3.687	0.7728	40.53
	TokenPure-s2	1.000	0.5136	1.000	0.0060	19.94	0.7880	0.2084	0.1781	3.218	0.7669	47.32
StegaStamp	TokenPure	1.000	0.4947	1.000	0.0080	21.19	0.8074	0.1920	0.1347	4.197	0.7743	33.34
	TokenPure-s4	1.000	0.5113	1.000	0.0120	20.61	0.8031	0.1952	0.1465	3.720	0.7728	37.40
	TokenPure-s2	1.000	0.5025	1.000	0.0080	20.34	0.7964	0.2093	0.1665	3.330	0.7703	44.92
StableSignature	TokenPure	0.9848	0.4677	0.9960	0.0065	18.02	0.6154	0.2891	0.1806	3.899	0.7399	37.91
	TokenPure-s4	0.9848	0.4481	0.9960	0.0059	17.10	0.6054	0.3006	0.1865	3.603	0.7449	42.41
	TokenPure-s2	0.9848	0.4654	0.9960	0.0092	16.77	0.6128	0.3431	0.2150	2.871	0.7404	47.03
TreeRing	TokenPure	1.000	0.7725	1.000	0.1850	17.81	0.6461	0.2661	0.1545	4.045	0.7333	34.97
	TokenPure-s4	1.000	0.8017	1.000	0.2662	17.28	0.6450	0.2890	0.1789	3.303	0.7329	38.30
	TokenPure-s2	1.000	0.8320	1.000	0.3300	17.08	0.6423	0.3119	0.1992	2.906	0.7350	42.68

More Qualitative results To further illustrate the superiority of TokenPure in visual consistency, we include additional visual comparisons in the supplementary materials (Figure 6), where each watermarking case presents the attacked image and a residual map (the difference between the attacked and original unwatermarked images).